

Supplement of Atmos. Chem. Phys., 18, 1363–1378, 2018  
<https://doi.org/10.5194/acp-18-1363-2018-supplement>  
© Author(s) 2018. This work is distributed under  
the Creative Commons Attribution 3.0 License.



*Supplement of*

## **Soil fluxes of carbonyl sulfide (COS), carbon monoxide, and carbon dioxide in a boreal forest in southern Finland**

**Wu Sun et al.**

*Correspondence to:* Wu Sun ([wu.sun@ucla.edu](mailto:wu.sun@ucla.edu)) and Ulli Seibt ([useibt@ucla.edu](mailto:useibt@ucla.edu))

The copyright of individual parts of the supplement might differ from the CC BY 3.0 License.

**Table S1.** Numbers of valid observations from the two chambers (SC1 and SC2).

	no. of total possible obs.			no. of missing obs.			no. of misfit obs. and outliers <sup>†</sup>			no. of valid obs.			% of valid obs.		
	SC1	SC2	both	SC1	SC2	both	SC1	SC2	both	SC1	SC2	both	SC1	SC2	both
$F_{\text{COS}}$	3768	1992	5760	143	98	241	549	859	1408	3076	1035	4111	81.63	51.96	71.37
$F_{\text{CO}}$	3768	1992	5760	143	98	241	601	870	1471	3024	1024	4048	80.25	51.41	70.28
$F_{\text{CO}_2}$	3768	1992	5760	143	98	241	544	868	1412	3081	1026	4107	81.77	51.51	71.30
$F_{\text{H}_2\text{O}}$	3768	1992	5760	143	98	241	534	854	1388	3091	1040	4131	82.03	52.21	71.72

<sup>†</sup>Misfits are measurements affected by severe instrument drift or fluctuation, whereas outliers are unusual peaks in the time series of the calculated fluxes identified from the Z-score statistic.

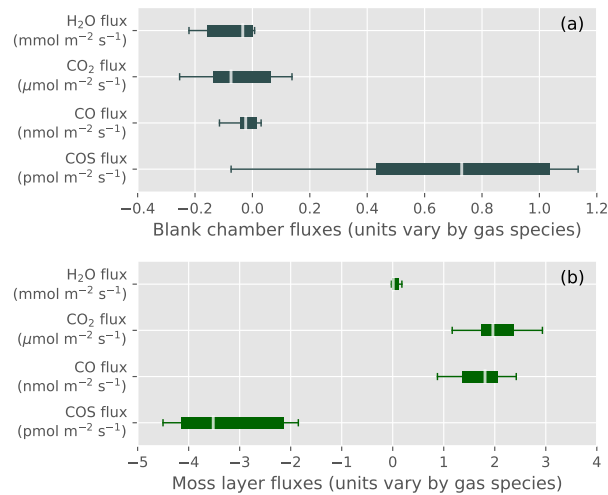


**Figure S1.** Boxplots of the fluxes of COS, CO, CO<sub>2</sub>, and H<sub>2</sub>O from (a) a blank chamber test for the apparent fluxes caused by chamber materials (see Sect. 2.2 in the main text), and from (b) an incubation of the moss layer in the field. Flux rates are normalized with respect to the chamber footprint area. For each flux term, the thin white bar marks the median value, the box represents the interquartile range, and the whiskers delimit the inlier range. Note that the units of fluxes differ by gas species, as shown on the y-axes.

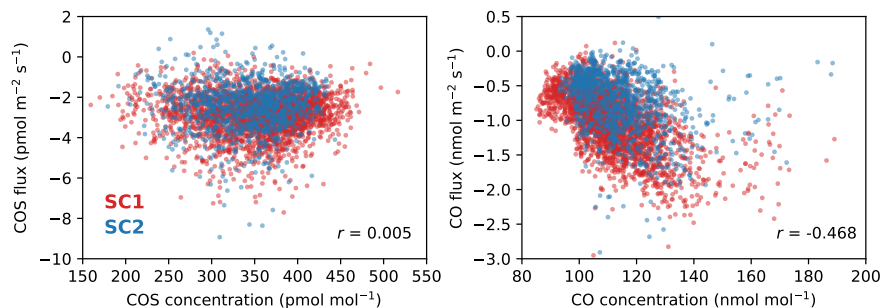


**Figure S2.** COS and CO fluxes versus their respective concentrations. COS uptake do not show a correlation with COS concentration ( $r = 0.005$ ,  $p = 0.738$ ), whereas CO uptake is weakly correlated with CO concentration ( $r = -0.468$ ,  $p < 1 \times 10^{-16}$ ).

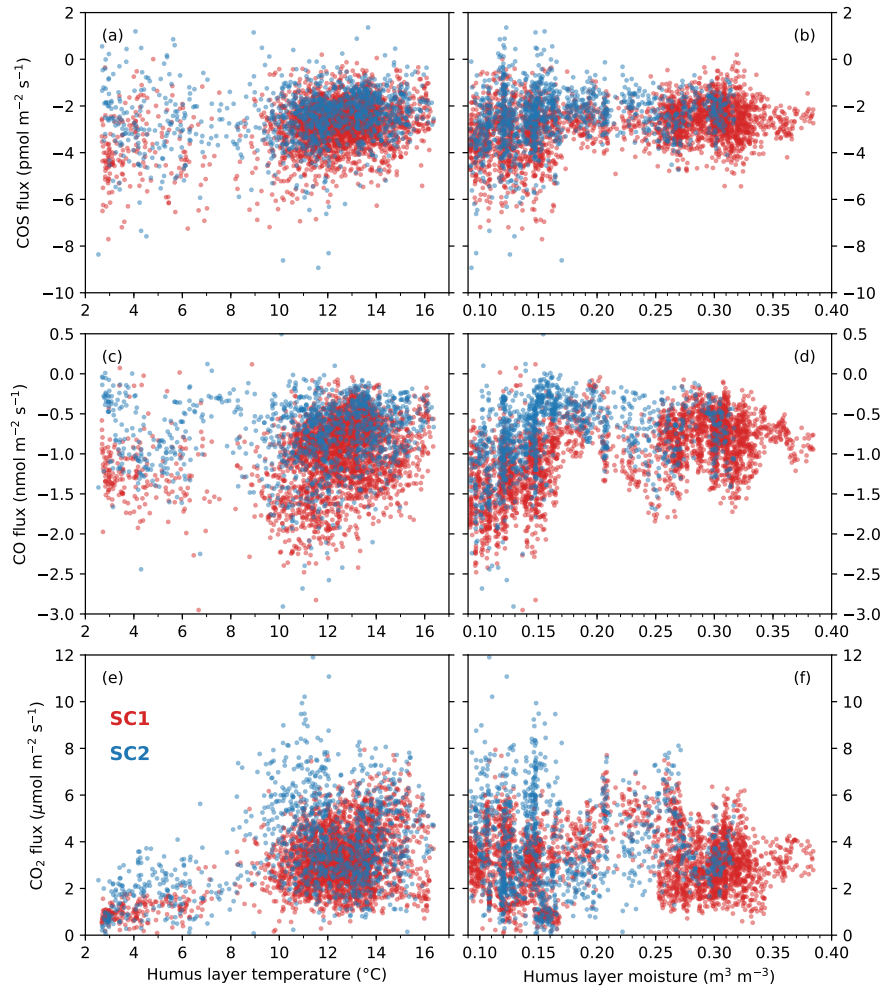


**Figure S3.** Soil fluxes of COS, CO, and CO<sub>2</sub> versus humus layer temperature and moisture.

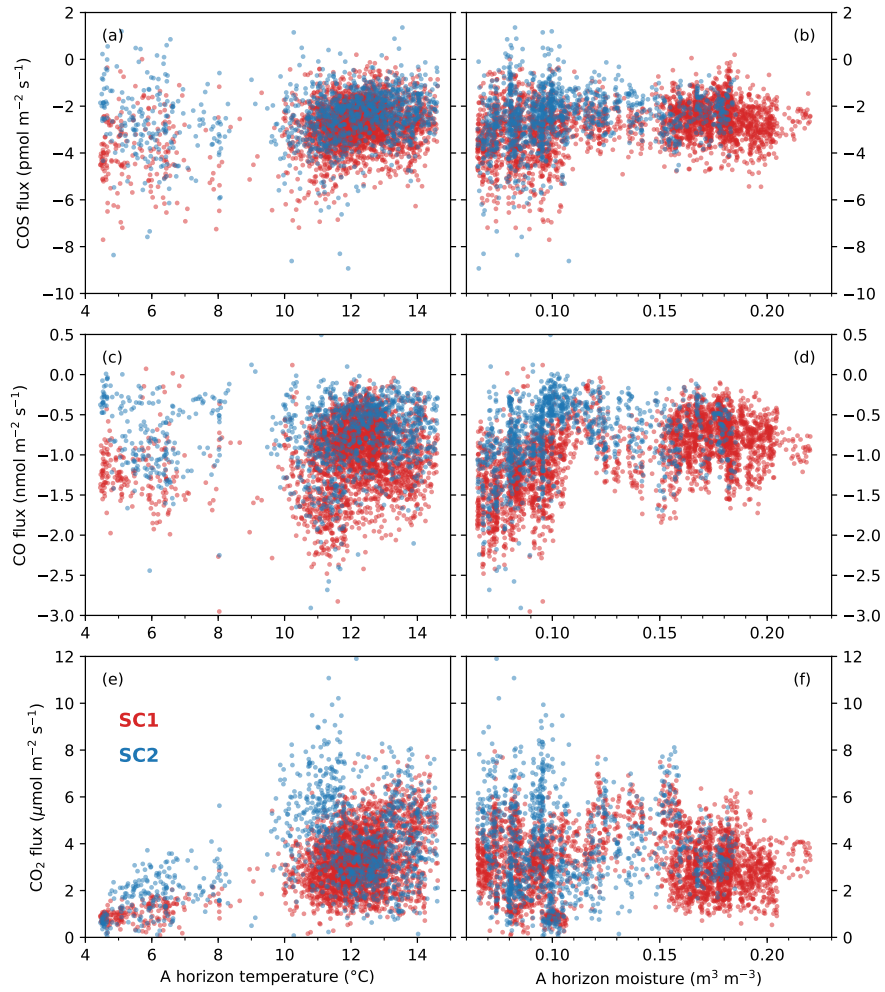


**Figure S4.** Soil fluxes of COS, CO, and CO<sub>2</sub> versus A horizon temperature and moisture.

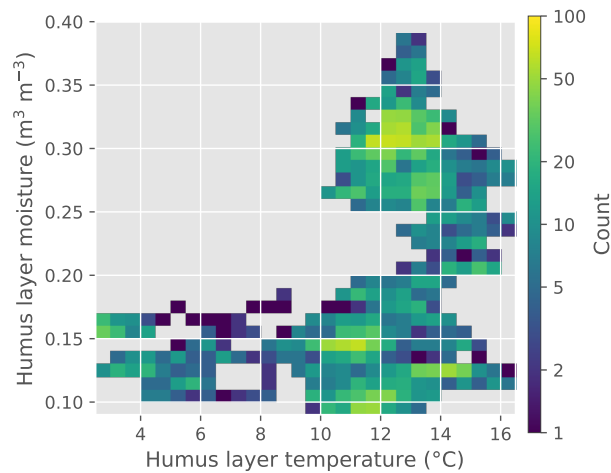


**Figure S5.** A 2D histogram for sample counts in temperature and moisture bins. Note that the scale is logarithmic for better visualization.

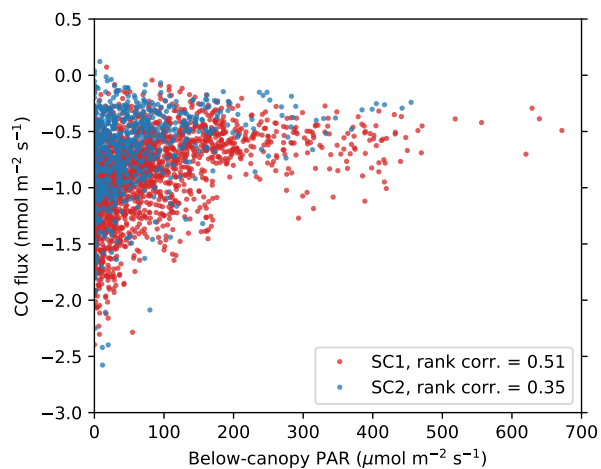


**Figure S6.** Daytime CO flux correlates weakly with below-canopy photosynthetically available radiation (PAR), as indicated by the Spearman's rank correlations shown on the figure legend.

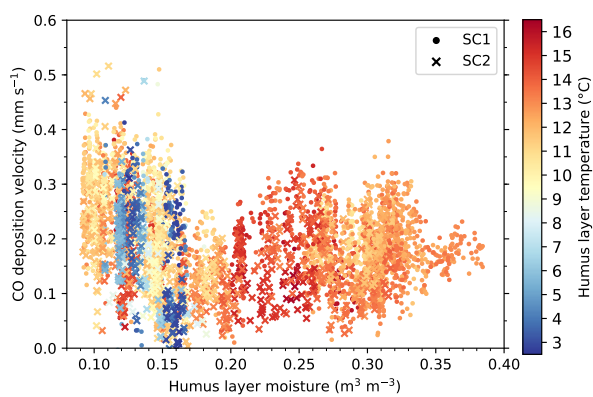


**Figure S7.** Apparent CO deposition velocity ( $-F_{\text{CO}}/[\text{CO}]_{0.5 \text{ m}}$ ) as a function of soil humus layer moisture ( $x$ -axis) and temperature (colors).

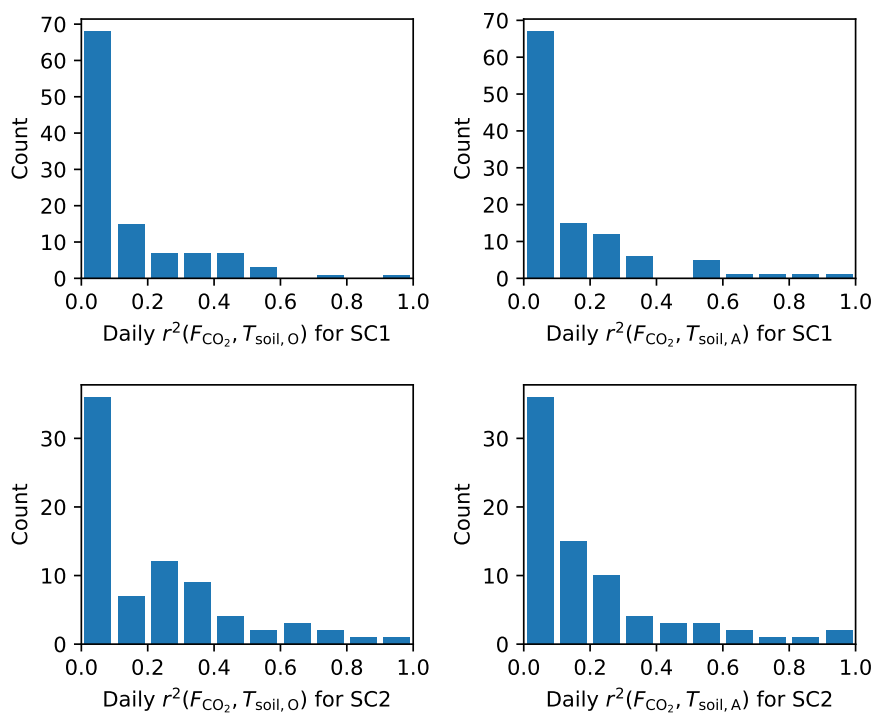


**Figure S8.** Histograms of the daily  $r^2$  values of the correlation between CO<sub>2</sub> flux and humus layer temperature (left column) or A horizon temperature (right column) for the two soil chambers (top row: SC1; bottom row: SC2). Most days showed insignificant or weak correlations between CO<sub>2</sub> flux and soil temperature variables.